

## **Resistivity Anisotropy Measured Using Four Probes in Epitaxial Graphene on Silicon Carbide**

Keisuke Kobayashi<sup>\*1</sup>, Shinichi Tanabe<sup>2</sup>, Takuto Tao<sup>1</sup>, Toshio Okumura<sup>1</sup>, Takeshi Nakashima<sup>1</sup>, Takuya Aritsuki<sup>1</sup>, Ryong-Sok O<sup>1</sup>, and Masao Nagase<sup>1</sup>

<sup>1</sup>*Graduate School of Advanced Technology and Science, The University of Tokushima, 2-1 Minamijyousanjima-cho, Tokushima 770-8506, Japan*

<sup>2</sup>*NTT Basic Research Laboratories, NTT Corporation, 3-1 Morinosato-Wakamiya, Atsugi, Kanagawa 243-0198, Japan*

E-mail: kobayashi@ee.tokushima-u.ac.jp

The electronic transport of epitaxial graphene on silicon carbide is anisotropic because of the anisotropy of the surface structure of the substrate. This letter presents a new method for measuring anisotropic transport based on the van der Pauw method. This method can measure anisotropic transport on the macroscopic scale without special equipment or device fabrication. We observe an anisotropic resistivity that has a ratio of maximum to minimum values of 1.62. The calculated maximum mobility is  $2876 \text{ cm}^2 \cdot \text{V}^{-1} \cdot \text{s}^{-1}$ , which is 1.43 times higher than that obtained with the standard van der Pauw method.

Graphene, a single atomic sheet of graphite, has attracted much attention because of its extraordinary properties.<sup>1,2)</sup> In particular, its mobility of  $200,000 \text{ cm}^2 \cdot \text{V}^{-1} \cdot \text{s}^{-1}$  is higher than that of any other material<sup>3)</sup>, which makes it a desirable material for making ultra-fast transistors.<sup>4)</sup> Producing large-area and high-quality graphene is required to support future industrial manufacturing. Thermal decomposition of silicon carbide (SiC) is the only method that can produce wafer-scale single-crystal graphene.<sup>5)</sup> In this method, the SiC substrate is annealed in an ultra-high vacuum<sup>6)</sup> or argon atmosphere.<sup>7)</sup> Silicon atoms sublime from the surface of the SiC substrate, and graphene is grown on the SiC substrate epitaxially.<sup>8)</sup> The CVD method<sup>9)</sup> can also obtain large area-graphene; however, the resulting graphene is polycrystalline. Furthermore, SiC is a semi-insulator, and graphene on SiC can be used for electronic devices<sup>10)</sup> without being transferred to another substrate, as in the case with CVD graphene on metal.

Graphene on SiC is grown on step-terrace structures<sup>11–13)</sup>, which cause anisotropic resistivity. In GaN<sup>14)</sup> and GaAs<sup>15)</sup>, anisotropic transport by step-terrace structures is observed by using device structures such as Hall bars and FET patterns. Similarly, in graphene on SiC, the transport characteristics are measured by using the device structure.<sup>16)</sup> Odaka et al. discussed the electronic transport in the directions parallel and perpendicular to the steps by fabricating FETs on the surface of the graphene.<sup>17)</sup> However, device fabrication influences the transport characteristics of graphene, and it is difficult to measure the dependence of the transport on angle in detail. Yakes et al. reported the microscopic transport anisotropy using an ultra-high vacuum (UHV) four-probe scanning tunneling microscope (STM).<sup>18)</sup> Nevertheless, the measurement is microscopic and requires expensive and complicated equipment.

In this letter, we discuss our new measurement method, which is based on the van der Pauw method for determining transport anisotropy.<sup>19)</sup> The van der Pauw method is a technique that measures the electronic transport properties of thin semiconductor materials. In this method, device fabrication is not needed. This is very advantageous because graphene is sensitive to the processes used to fabricate devices, such as the resist process in photolithography. The method based on the van der Pauw method is a nondestructive measurement for a given device area and provides macroscopic information about an entire sample. Moreover, this method requires no special equipment. In previous work<sup>20)</sup>, the van der Pauw method using four probes had been used for anisotropic resistivity measurements in the parallel and perpendicular directions. Here, the detailed angular dependence of the anisotropic resistivity will be discussed.

Figure 1(a) shows the arrangement of probes of the standard van der Pauw method for a square sample. Four probes are placed at the corners of the square. First, the currents  $I_{\rho 1}$  and  $I_{\rho 2}$  are applied to the sides of square to perform a resistivity measurement. Second, the current  $I_H$  is applied in the diagonal direction to perform a Hall voltage measurement. The direction of the current  $I_{\rho 1}$  is perpendicular to the direction of the current  $I_{\rho 2}$ . Therefore, the anisotropic resistivity of the sample is canceled. The conventional method has the limitation that it must be applied to an isotropic sample. Therefore, the standard van der Pauw method can not measure the anisotropic transport properties of graphene on SiC. For this reason, we improved the standard van der Pauw method, resulting in a new method that we call the aligned van der Pauw method, which can measure anisotropic samples.

Figure 1(b) shows the arrangement of probes employed in the aligned van der Pauw method. Each side of the square is divided into  $N$  parts, and four probes are placed on the edge of the sample. The positions of the probes at the corners are labeled  $A_1$ – $D_1$ , and moving from each of these positions to the next clockwise location (where these probe locations are marked by circles in Fig. 1(b)), the other probe positions are labeled  $A_n$ – $D_n$  (where  $n = 1, 2, 3, \dots, N$ ). The measurement is carried out with these four probes at each of the sets of locations  $A_n$ – $D_n$ . The measurements of the resistivity and Hall voltage using the four probes are repeated  $N$  times (once for each of the  $N$  distinct probe configurations). The distinctive feature of the aligned van der Pauw method is the calculation method employed after the measurement. The direction of the current used for calculating resistivity and that for calculating the Hall voltage must be almost aligned with each other. For example, in the case shown in Fig. 1(b), the resistivity is calculated by using a pair of currents  $I_{\rho 1}$  and  $I_{\rho 2}$  of the same angle. Then, the Hall voltage must be calculated by using a current  $I_H$  that has a similar direction. Thereby, the anisotropic resistivity is not canceled, and the intrinsic resistivity and mobility are calculated. In this letter, we divide the side of the sample into  $N = 4$  segments. We defined the direction of the current for measuring the Hall voltage (the Hall measurement current angle) as  $\theta$  and a side of the sample as  $\theta = 0^\circ$ . The angles of the measurement are between  $90^\circ$  and  $-90^\circ$ . In addition, we note that the current polarity is changed to reduce the measurement error, and each resistivity value is calculated by using four measured resistance values.

We compared the aligned van der Pauw method to the standard van der Pauw method with the same sample. The sample was fabricated from a 4H-SiC(0001) substrate manufactured by Cree Inc., and was diced into exact squares of size  $10 \times 10$  mm by stealth dicing.<sup>21)</sup> The direction of  $\theta = 0^\circ$  is  $\langle 1100 \rangle$ . The annealing condition is 10 minutes at

1620 °C under a pressure of 100 Torr in an argon atmosphere. The sample was identified by an atomic force microscope (AFM) and a Raman spectroscopy.<sup>22)</sup> The sample was covered with single-layer graphene and was homogeneous on the scale of the wafer. For the probes, we used the Ecopia SPCB-01; we used a Keithley 2430 as the measurement instrument and a pair of neodymium magnets to apply the magnetic field. The applied magnetic field had a strength of 261 mT.

Figure 2 shows the comparison of resistivity between the aligned van der Pauw method and the standard van der Pauw method. The resistivity was measured by the standard van der Pauw method and was found to be almost constant. As explained above, the anisotropy of the resistivity is canceled in this scheme. In contrast, the anisotropy of the resistivity could be measured by the aligned van der Pauw method. The resistivity took its maximum value of  $1.20 \times 10^{-4} \Omega \cdot \text{cm}$  at  $45^\circ$ , and the corresponding minimum was  $7.40 \times 10^{-5} \Omega \cdot \text{cm}$  at  $-45^\circ$ . The topographical image from the AFM suggests that the resistivity tends to the minimum value when the current is parallel to the steps, and the maximum occurs when the current is perpendicular to the steps. This result corresponds with that of Odaka et al.<sup>17)</sup> The curve was computed based on the results of calculations with the SPICE (Simulation Program with Integrated Circuit Emphasis) software package.<sup>23)</sup> In this simulation, two types of resistors are connected with each other, forming a lattice. These resistors play the roles of step and terrace, thus reproducing the step-terrace structure. Versnel<sup>24)</sup> reported that the shape effect of the resistivity in the van der Pauw method can be neglected for squares. Therefore, this result of resistivity does not include the shape effect, and the intrinsic resistivity can be measured.

Figure 3 shows a comparison of values of the factor  $f$ , which is a dimensionless function of only the measured resistance values. In Fig. 3, according to the van der Pauw method<sup>19)</sup>, the values of  $f$  are given by the expression

$$f \approx 1 - \left( \frac{R_{\rho 1} - R_{\rho 2}}{R_{\rho 1} + R_{\rho 2}} \right)^2 \frac{\ln 2}{2} - \left( \frac{R_{\rho 1} - R_{\rho 2}}{R_{\rho 1} + R_{\rho 2}} \right)^4 \left[ \frac{(\ln 2)^2}{4} - \frac{(\ln 2)^3}{12} \right], \quad (1)$$

where the resistance value is calculated from the current and the voltage in Fig. 1 ( $R_{\rho 1} = V_{\rho 1}/I_{\rho 1}$  and  $R_{\rho 2} = V_{\rho 2}/I_{\rho 2}$ ). Under the arrangement of probes shown Fig. 1(b), this  $f$  is one when the sample and measurement are ideal. The value of  $f$  in the standard van der Pauw method is below one (having an average of 0.977) because the sample is anisotropic. In contrast, the value of  $f$  in the aligned van der Pauw method is stable and exactly one (with an average of 1.00) because the sample is exactly square and the thickness of the graphene

film is highly uniform over the entire sample. Hence, this result also indicates that the aligned van der Pauw method can measure the anisotropic resistivity correctly.

Figure 4 shows the mobility and sheet carrier density in the aligned van der Pauw method. The curve is obtained by using the simulated resistivity (see Fig. 2) and the average of the measured sheet carrier density. In the standard van der Pauw method, the average of the mobility was  $2009 \text{ cm}^2 \cdot \text{V}^{-1} \cdot \text{s}^{-1}$ . By contrast, in the aligned van der Pauw method, the maximum mobility is  $2876 \text{ cm}^2 \cdot \text{V}^{-1} \cdot \text{s}^{-1}$  at  $-45^\circ$ . The estimates resulting from these two methods therefore differ by a factor of 1.43. Consequently, in contrast to the resistivity, the mobility takes its maximum value when the current is parallel to the steps, and the minimum occurs when the current is perpendicular to the steps. It is clear that the mobility of graphene on SiC is underestimated when it is measured by using the standard van der Pauw method. The sheet carrier density is the same in both methods because both methods use the same arrangement of probes.

Finally, we note that modifying the shape of the device to circular can allow more precise measurements to be performed. If the sample is round, the measurement angle is easily determined. In this method, probes are required to be placed every  $45^\circ$ , and a larger value of  $N$  (e.g., 10, 18, and 30) should be employed for more precise measurement. Thereby, the angle of the current used to measure the resistivity becomes just the same as that for the Hall voltage. For example, in the case of  $N = 18$  (72 probes) and a sample diameter of 10 mm, the probe pitch should be approximately  $436 \mu\text{m}$ . A special instrument with multiple probes to implement the aligned van der Pauw method will be realized to allow efficient measurement.

In conclusion, we proposed a new method called the aligned van der Pauw method for performing anisotropic resistivity measurements. The anisotropy of the resistivity is 1.62 times the ratio between maximum and minimum for monolayer graphene on SiC. The calculated anisotropic mobility is  $2876 \text{ cm}^2 \cdot \text{V}^{-1} \cdot \text{s}^{-1}$  at maximum. The results of the measurement prove that our aligned van der Pauw method is a useful means of measuring an anisotropic material such as graphene on SiC with a step-terrace structure. Being able to perform such measurements simply, quickly, and easily by using the aligned van der Pauw method will facilitate the application of graphene to future electronic devices.

## **Acknowledgement**

The authors thank Dr. H. Hibino of NTT Basic Research Laboratories and Dr. Y. Ohno of the University of Tokushima for their helpful discussions. This work was partially supported by JSPS KAKENHI Grant Number 26289107.

## References

- 1) K. S. Novoselov, A. K. Geim, S. V. Morozov, D. Jiang, Y. Zhang, S. V. Dubonos, I. V. Grigorieva, and A. A. Firsov, *Science* **306**, 666 (2004).
- 2) K. S. Novoselov, A. K. Geim, S. V. Morozov, D. Jiang, M. I. Katsnelson, I. V. Grigorieva, S. V. Dubonos, and A. A. Firsov, *Nature* **438**, 197 (2005).
- 3) K. I. Bolotin, K. J. Sikes, Z. Jiang, M. Klima, G. Fudenberg, J. Hone, P. Kim, and H. L. Stormer, *Solid State Commun.* **146**, 351 (2008).
- 4) Y.-M. Lin, C. Dimitrakopoulos, K. A. Jenkins, D. B. Farmer, H.-Y. Chiu, A. Grill, and Ph. Avouris, *Science* **327**, 662 (2010).
- 5) C. Berger, Z. Song, T. Li, X. Li, A. Y. Ogbazghi, R. Feng, Z. Dai, A. N. Marchenkov, E. H. Conrad, P. N. First, and W. A. de Heer, *J. Phys. Chem. B* **108**, 19912 (2004).
- 6) J. Hass, W. A. de Heer, and E. H. Conrad, *J. Phys.: Condens. Matter.* **20**, 323202 (2008).
- 7) K. V. Emtsev, A. Bostwick, K. Horn, J. Jobst, G. L. Kellogg, L. Ley, J. L. McChesney, T. Ohta, S. A. Reshanov, J. Röhrl, E. Rotenberg, A. K. Schmid, D. Waldmann, H. B. Weber, and T. Seyller, *Nat. Mater.* **8**, 203 (2009).
- 8) H. Hibino, H. Kageshima, and M. Nagase, *J. Phys. D: Appl. Phys.* **43**, 374005 (2010).
- 9) X. Li, W. Cai, J. An, S. Kim, J. Nah, D. Yang, R. Piner, A. Velamakanni, I. Jung, E. Tutuc, S. K. Banerjee, L. Colombo, and R. S. Ruoff, *Science* **324**, 1312 (2009).
- 10) S. Tanabe, Y. Sekine, H. Kageshima, M. Nagase, and H. Hibino, *Appl. Phys. Express* **3**, 075102 (2010).
- 11) S.-H. Ji, J. B. Hannon, R. M. Tromp, V. Perebeinos, J. Tersoff, and F. M. Ross, *Nat. Mater.* **11**, 114 (2012).
- 12) T. Low, V. Perebeinos, J. Tersoff, and Ph. Avouris, *Phys. Rev. Lett.* **108**, 096601 (2012).
- 13) M. Nagase, H. Hibino, H. Kageshima, and H. Yamaguchi, *Appl. Phys. Express* **6**, 055101 (2013).
- 14) N. Nakamura, K. Furuta, X. Q. Shen, T. Kitamura, K. Nakamura, and H. Okumura, *J. Cryst. Growth* **301-302**, 452 (2007).
- 15) M. Akabori, J. Motohisa, and T. Fukui, *J. Cryst. Growth* **195**, 579 (1998).
- 16) Y.-M. Lin, D. B. Farmer, K. A. Jenkins, Y. Wu, J. L. Tedesco, R. L. Myers-Ward, C. R. Eddy, Jr., D. K. Gaskill, C. Dimitrakopoulos, and P. Avouris, *IEEE Electron Device Lett.* **32**, 1343 (2011).
- 17) S. Odaka, H. Miyazaki, S.-L. Li, A. Kanda, K. Morita, S. Tanaka, Y. Miyata, H. Kataura, K. Tsukagoshi, and Y. Aoyagi, *Appl. Phys. Lett.* **96**, 062111 (2010).

- 18) M. K. Yakes, D. Gunlycke, J. L. Tedesco, P. M. Campbell, R. L. Myers-Ward, C. R. Eddy, Jr., D. K. Gaskill, P. E. Sheehan, and A. R. Laracuente, *Nano Lett.* **10**, 1559 (2010).
- 19) L. J. van der Pauw, *Philips Res. Rep.* **13**, 1 (1958).
- 20) O. Bierwagen, R. Pomraenke, S. Eilers, and W. T. Masselink, *Phys. Rev. B* **70**, 165307 (2004).
- 21) E. Ohmura, F. Fukuyo, K. Fukumitsu, and H. Morita, *Journal of Achievements in Materials and Manufacturing Engineering* **17**, 381 (2006).
- 22) R. O, A. Iwamoto, Y. Nishi, Y. Funase, T. Yuasa, T. Tomita, M. Nagase, H. Hibino, and H. Yamaguchi, *Jpn. J. Appl. Phys.* **51**, 06FD06 (2012).
- 23) L. W. Nagel, Memorandum No. ERL-M520, University of California, Berkeley (1975).
- 24) W. Versnel, *Solid-State Electron.* **21**, 1261 (1978).



## Figure Captions

**Fig. 1.** (Color online) Schematic of the arrangement of probes for a square sample. (a) Standard van der Pauw method. (b) Aligned van der Pauw method.

**Fig. 2.** (Color online) Comparison of the dependences of the measured resistivity on the Hall measurement current angle for the standard and aligned van der Pauw methods. The red solid line is the simulated step-terrace resistivity. The inset is a topographical image of the sample from the AFM.

**Fig. 3.** (Color online) Comparison of the factor  $f$  (a dimensionless function of only the measured resistance values) under the standard and aligned van der Pauw methods.

**Fig. 4.** (Color online) Dependences of the mobility and sheet carrier density on the Hall measurement current angle in the aligned van der Pauw method. The red solid line is the simulated results obtained by using SPICE.

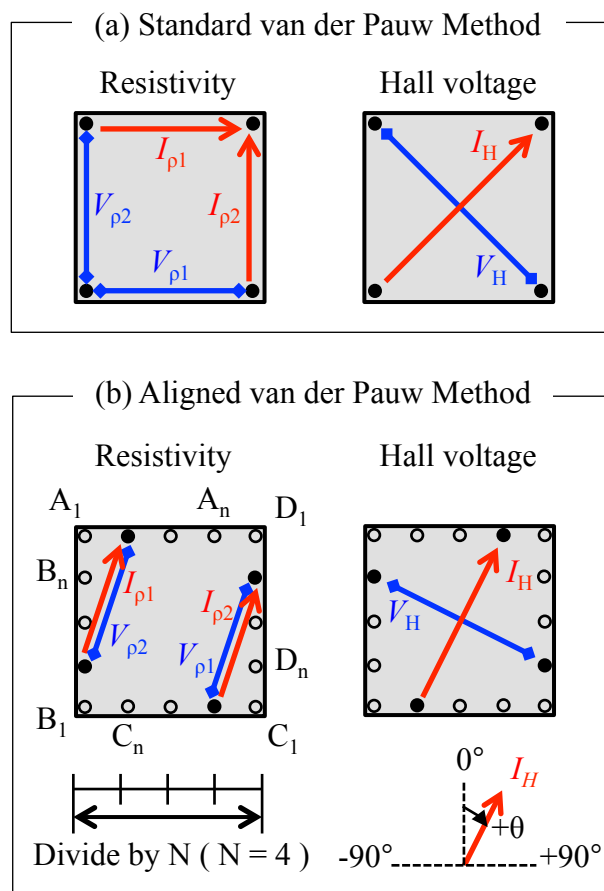


Fig. 1.

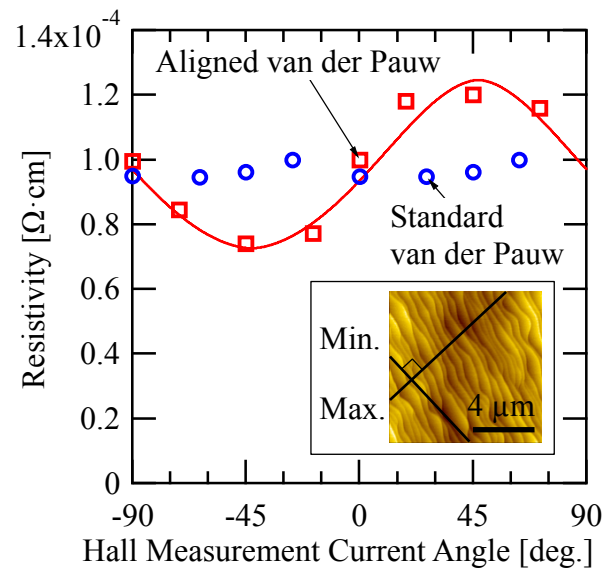


Fig. 2.

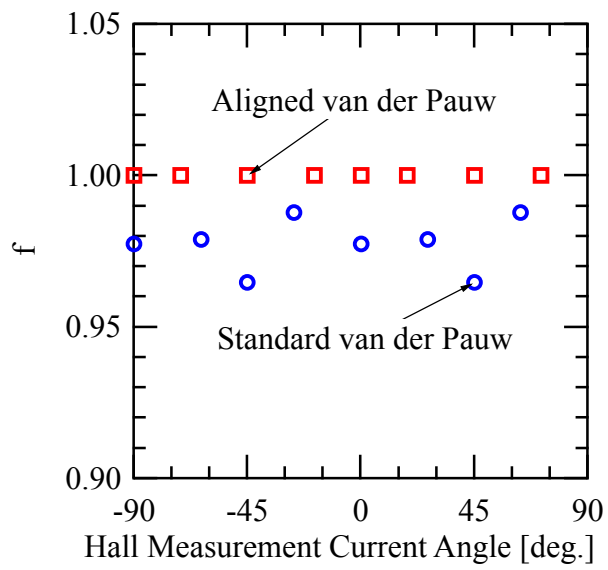


Fig. 3.

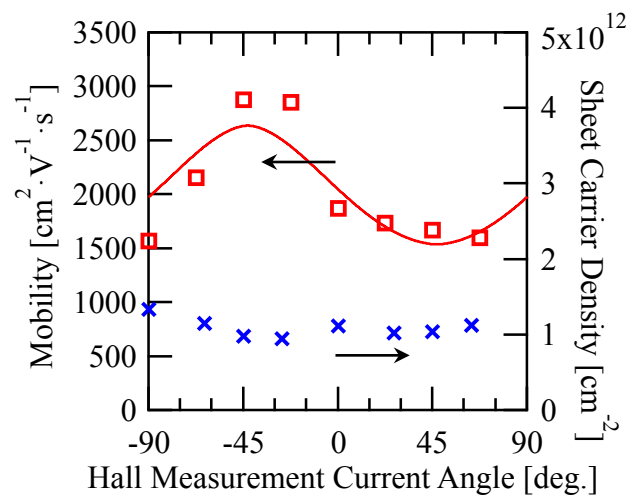


Fig. 4.